crystals

MDPI

Article

Fusion–Extraction Technique of Vanadium(III) Using Ammonium Phosphate Salt as Flux

Trevor T. Chiweshe

Institute for Groundwater Studies, University of the Free State, Nelson Mandela Drive, Bloemfontein 9300, South Africa; chiweshetrevor@gmail.com

Abstract: This study presents an alternative fusion method for sample dissolution and extraction of vanadium from an inorganic (V_2O_3) compound and mineral ore sample (AMIS 0501) using phosphate salts as flux. Complete sample dissolution was achieved at 800 °C within ±20 min using both the sodium and ammonium phosphate flux. The precipitation of vanadium was subsequently achieved after the fusion of the sample using ammonium phosphate flux, and no precipitate was obtained using sodium phosphate flux. The differences in cations between the two fluxes (NH_4^+ and Na^+) influenced the precipitation of vanadium. The XRD analysis of the precipitate from V_2O_3 using ammonium phosphate showed a monoclinic structure of vanadium (III) tris(metaphosphate) ($V(PO_3)_3$) compound, which belonged to the *Ic* space group with lattice parameters a = 10.6071, b = 19.0871 and c = 9.4230. A remarkable vanadium recovery of 98% was obtained from inorganic compounds, V_2O_3, and up to 70% from the AMIS mineral ore sample using the ammonium phosphate flux method. The vanadium precipitates from AMIS contained Fe (20.97%) and Ti (44.97%), which occurred as impurities in the recovery of vanadium using the ammonium phosphate flux method.

Keywords: vanadium(III) tris(metaphosphate); ammonium and sodium phosphate flux; vanadium(III) oxide; fusion technique

Citation: Chiweshe, T.T. Fusion–Extraction Technique of Vanadium(III) Using Ammonium Phosphate Salt as Flux. *Crystals* **2022**, *12*, 1464. https://doi.org/10.3390/cryst12101464

Academic Editors: Yufeng Guo, Shuai Wang, Feng Chen, Lingzhi Yang, Yulei Sui and Hongyang Wang

Received: 13 September 2022
Accepted: 12 October 2022
Published: 17 October 2022

1. Introduction

Vanadium reserves are estimated to be ±63 million metric tons (Mt) in the world, and the major producing countries include China, Russia, and South Africa, accounting for approximately 98% of the world's production. Titanomagnetite is the principal source of vanadium in the world and is also one of the major sources of iron and titanium [1]. In South Africa, vanadium-bearing titaniferous magnetite (titanomagnetite) is mined in the northern and western limbs of the Bushveld Igneous Complex (BIC). The titanomagnetite strata in the BIC range from 0.12 to 10 m thickness and contain approximately 50–58% (Fe_2O_3), 10–25% (TiO_2), and 0.2–2.0% (V_2O_5) [2]. Some of the noble properties of vanadium, which makes it indispensable in chemical and steel industries, is its ability to resist corrosion as well as alkali and acid attack. Vanadium is classified as a 'critical mineral' in the steel industry and is used to improve both tensile strength and toughness in steelmaking, which accounts for up to 93% of consumption. The chemical industry accounts for 3% of vanadium consumption and is mostly used as catalysts [3] and in the production of ferrovanadium alloy (~4%) due to its high strength-to-weight ratio, weldability, and formability [4]. The estimated consumption rate of vanadium is expected to surge due to an increase in demand by the steel industry. The recent developments in the battery industry show an increase in vanadium use in the production of vanadium redox batteries (VRBs) (~0.1%) used for storing renewable sources of energy [5].

The increased demand for vanadium products, especially in the battery sector, is set to increase considerably as producers shift away from the ever-increasing cost of the key component, lithium. However, the metallurgical extraction of vanadium from ore is complicated by several factors, which include low abundance (<1%), unreliable ore

processing techniques, and the formation of refractory compounds limiting the production of vanadium. Modern techniques use smelting as a method of choice to extract vanadium as a byproduct. High temperatures are usually employed to evade the formation of infusible and refractory compounds that may interfere with the furnace operation. These compounds limit the normal operating conditions of the blast furnace by forming sticky melts, which cause high operational costs and frequent shutdown of plants [6]. Studies show the effects of refractory compounds in minimizing vanadium concentrations in the slags used as feed for vanadium processing [7]. Some studies have attempted to recover vanadium using various approaches from these slags, but most of the developed techniques [8] suffer from sensitivity and selectivity issues, which resulted in unsatisfactory recoveries. The modern alternative for recovering vanadium from slags is by a roasting-assisted leaching process, followed by hydrometallurgical separation or purification and recovery as a metal or oxide (V_2O_5), ferrovanadium or any other compound, depending on the method used [9]. The biggest challenges using this method are the high energy demand required by this process to achieve the best recoveries as well as the time needed to complete the separation procedure.

In pyrometallurgical processes, the nature of the vanadium ore plays a critical role in the determination of the best approach for extraction, as most of the vanadium-bearing slags contain impurities such as Fe, Ti, Mn, Cr, etc. Magnetite (Fe_3O_4) and ilmenite ($FeTiO_3$) are the major sources of Fe and Ti, and these mineral phases are interlinked, which makes it difficult to achieve a clean separation using physical beneficiation processes. Another challenge in the beneficiation process is the presence of chromium in the ore. Chromium forms isomorphous compounds with vanadium, which complicates the extraction process due to similar chemical properties. Some of the techniques used to optimize the percentage recoveries in titanomagnetite include the reduction in ilmenite content by 10–15%, which is estimated to increase the vanadium content by approximately 1.5% in the magnetic fraction (Fe_3O_4). Research studies have established and improved selective separation methods for vanadium from its naturally occurring impurities such as Fe, Ti, and Cr by using precipitation methods, [10] ion exchange, solvent extraction [11], and selective adsorption using activated carbon and ionic liquids [12].

The current work originated from our previous study [13], where microcrystalline C-type chromium(III) tris(metaphosphate), $Cr(PO_3)_3$ (JCPDS # 01-077-0672) [14,15] was isolated using the ammonium phosphate fusion technique. The similarity between the crystal structure of chromium(III) tris(metaphosphate) and vanadium(III) tris(metaphosphate) (isomorphs) [16,17] prompted the search for an alternative selective approach for vanadium extraction. Although various forms of vanadium phosphate compounds ($V(PO_3)_3$, $VO(PO_3)_2$, VPO_5, and $(VO)_2P_2O_7$) have been reported, it still remains to be determined if the fusion method using ammonium phosphate salt can result in the selective isolation of vanadium from the naturally occurring contaminants [5,18]. In this study, we examined the use of ammonium phosphate salt as a flux in the extraction of vanadium from an inorganic compound (V_2O_3) and mineral ore sample (AMIS 0501). A comparative study using sodium phosphate salt as the flux was performed to determine the influence of cations (NH_4^+ and Na^+) in the dissolution and selective separation of vanadium. The characterization of the vanadium solid products was achieved using infrared (IR), scanning electron microscopy–energy-dispersive X-ray spectroscopy (SEM-EDX), transmission emission microscopy (TEM), and X-ray diffractive (XRD) spectroscopy, whilst inductive coupled plasma–mass spectroscopy (ICP-MS) was used for the wet chemical analysis of the filtrate solution.

2. Experimental

2.1. Chemicals and Materials

Ammonium hydrogen phosphate ($(NH_4)_2HPO_4$ and $(NH_4)H_2PO_4$) (99%), sodium hydrogen phosphate ((Na_2HPO_4) and (NaH_2PO_4)) (99%), and vanadium (III) oxide (V_2O_3) were purchased from Merck Chemicals. The original vanadium multielement ICP standard (1000 mg/L), together with the mineral acids (HCl, 32%) and (HNO_3 65%), were also

purchased from Merck Chemicals. The ceramic crucibles (capacity, 100 mL) were supplied by Lasec SA, and all the reagents were used without further purification. Ultra-pure deionized water (0.01 μS/cm, conductivity) was used for wet chemical analysis, and all the analytical experimental measurements were reported as averages of three replicates.

2.2. Description of the Reference Standard Used as a Mineral Ore Sample

The reference standard used as a mineral ore sample in this study was AMIS 0501 (100 g), which was purchased from African Mineral Standards (AMIS). According to the analysis certificate, the reference material originated from the Mapochs mine in the Limpopo Province and was taken from a stockpile, which was mined from the main magnetite layer on the eastern Bushveld limb. The material was crushed, dry-milled, and then air-classified to less than 54 microns. The confirmation of particle size was achieved using wet sieve particle size analysis, which confirmed the material contained 98.5% of particles less than 54 microns. The certified elemental content of the major elements in the sample were reported as 53.76 ± 0.72% (Fe), 7.67 ± 0.57% (Ti), and 0.971 ± 0.076% (V).

2.3. Equipment

The fusion of the vanadium oxide and mineral ore (AMIS 0501) was conducted using a Barnstead Thermolyne furnace. A Eutech pH meter (CyberScan, pH 1500) was used for the pH measurements of the filtrate solutions. The characterization of the solid products was achieved using an IR spectrometer, Digilab (FTS 2000 model), EDX (Oxford X-Max^N) equipped with an SEM (Tescan VEGA3) from the Centre for Microscopy (University of the Free State), and XRD (D8 Advance Bruker) from the Physics Department (University of the Free State). A wet chemical analysis was performed using a PerkinElmer Nexion (model 2000c) ICP Mass spectrometer using the measurement conditions listed in Table 1.

Table 1. Selected ICP-MS operating conditions for elemental analysis using the KED mode.

Parameter/Component	Value/Type/Mode
Nebulizer gas flow	0.96 L/min
Auxiliary gas flow	1.2 L/min
RF power	1100 W
Plasma gas flow	15 L/min
Rinsing time	60 s
Nebulizer	Meinhard concentric type A3
Spray chamber	Baffled quartz cyclonic
Scanning mode	Peak hopping
Dwell time	50 ms
Replicates	3
Integration time	1 s/mas
Torch position	X (−1.52 mm), Y (−0.33 mm), and Z (0.00 mm)
Mode of operation	Kinetic discrimination energy (KED) using Helium gas

2.4. Preparation of Multielement Calibration Standards

Multielement calibration standards with a working range of 0–500 μg/L were prepared in separate volumetric flasks (100.0 mL) using a 'Transferpette' micropipette. The solutions were acidified using HCl (5.0 mL; 32%) and filled to the mark using deionized water. The final solutions were homogenized before use.

2.5. Fusion of Vanadium Oxide and Mineral Ore (AMIS 0501) Using Ammonium and Sodium Phosphate Salt

The fusion of vanadium oxide (V_2O_3) and AMIS mineral ore were conducted separately in triplicate analyses using ammonium phosphate ($(NH_4)_2HPO_4/(NH_4)H_2PO_4$) and

sodium phosphate salt (H_2NaPO_4/HNa_2PO_4), as shown in Scheme 1. Powdered samples of vanadium oxide (V_2O_3) and AMIS mineral ore (1.0 g) were thoroughly mixed in separate ceramic crucibles with an excess amount of ammonium phosphate and sodium phosphate salt (sample: flux ratio, 1:25). The resultant mixtures were heated in a furnace (800 °C) until molten melts were formed (±15 min). The red-hot molten melts were cooled at room temperature, and deionized water (50 mL) was added. The solid melts were stirred until all the melts were dissolved (sodium phosphate) and formed a precipitate (ammonium phosphate). The mixture of the ammonium phosphate flux was filtered, and the solid product was air-dried at room temperature and characterized using IR, SEM-EDX, and XRD analyses, whilst the filtrate was analyzed using ICP-MS.

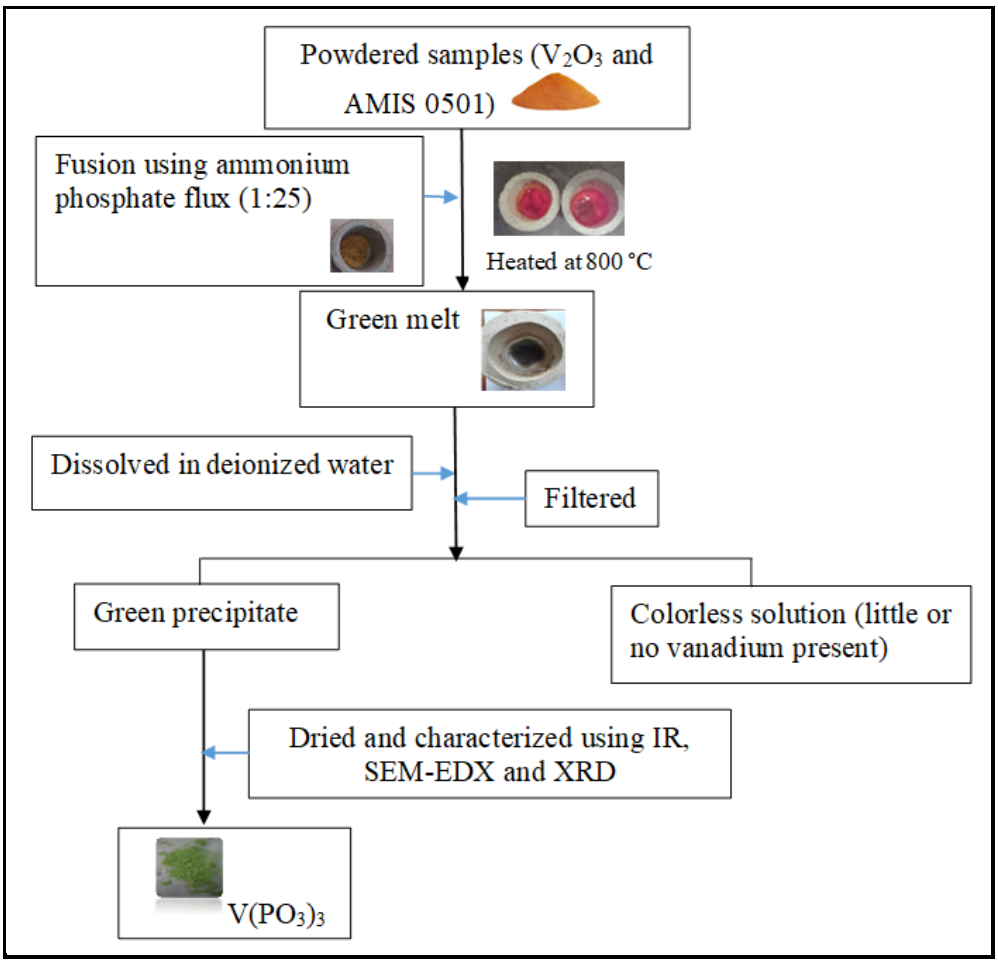

Scheme 1. A summary of fusion process using ammonium phosphate flux and the isolation of vanadium as vanadium(III) tris(metaphosphate) from V_2O_3 and AMIS 0501 mineral ore: IR, infrared; SEM-EDX, scanning electron microscopy–energy-dispersive X-ray spectroscopy; XRD, X-ray diffractive spectroscopy.

2.6. Analysis of the Precipitate Obtained Using Ammonium Phosphate Flux

2.6.1. SEM-EDX and TEM Analyses

SEM Analysis

The material was mounted on aluminum pin stubs using double-sided carbon tape and coated with iridium (±10 nm) using a Leica EM ACE600 sputter coater. The specimens were imaged and analyzed with a JSM-7800F Extreme-Resolution Analytical Field-Emission SEM (Tokyo, Japan), equipped with an Oxford Instruments X-Max 80 mm EDS detector, using the AZtec software. The samples were imaged at 5 kV at a WD of 10 mm, and EDS analyses were performed at 10 or 20 kV.

TEM Analysis

The samples were dispersed in methanol, and a drop was placed on a copper formvar grid to dry. The specimens were examined with a Philips CM100 TEM (FEI, Eindhoven, The Netherlands) at 60 kV.

XRD Analysis

The XRD analysis was used for the phase identification of the vanadium precipitate obtained from V_2O_3. A Bruker (D8 Focus model) X-ray diffractometer equipped with Cu K_α radiation of wavelength $\approx$ 0.154 nm was used to record the XRD patterns. Rietveld refinement was performed using the FullProf software to calculate structural parameters.

2.7. Analysis of the Filtrate Solutions Obtained Using Both Sodium and Ammonium Phosphate Flux

ICP-MS Analysis

ICP-MS was used to determine the elemental content of the filtrate solutions obtained after the fusion of vanadium oxide and mineral ore (AMIS 0501) using sodium phosphate and ammonium phosphate fluxes. The excess sodium content in the filtrate solutions obtained from sodium phosphate was removed as colorless crystals (confirmed as sodium chloride) by adding HCl (20 mL; 32%) and allowing the solution to stand overnight.

3. Results and Discussion

The extraction process of vanadium from V_2O_3 and mineral ore was conducted in three stages: (i) the fusion of the sample using ammonium and sodium phosphate salt, (ii) the dissolution of the melt, and (iii) the separation of the solid precipitate from the solution. The fusion stage was critical for the successful conversion of the starting material into a molten melt to achieve the complete liberation of the elemental components of the sample. The complete dissolution of the melt (intermediate product), as well as the target element, was achieved using deionized water. The final stage involved the separation of the desired products from impurities based on solubility differences. Vanadium-containing compounds instantly precipitated after the dissolution of the melt in deionized water. The fusion procedure was initially tested on pure inorganic vanadium oxide (V_2O_3) to determine the feasibility and efficiency of this method. The fusion of V_2O_3 and AMIS 0501 mineral ore was first assessed with ammonium phosphate salt flux using moderate temperatures (800 °C). Complete sample conversion was achieved within minutes ($\pm$15 min), and the melts appeared shiny and glassy. The hardness of the melts ranged between 6 and 7 according to the Mohs hardness test [19]. The solid melts were both soluble in deionized water but insoluble in most organic and inorganic solvents. Highly acidic solution pH (1.2–1.8) remained after the dissolution of both solid melts in deionized water, which was accompanied by the instant precipitation of a microcrystalline green product and powdered grey product from V_2O_3 and AMIS 0501, respectively. Both solid precipitates were insoluble in most common mineral acids even in organic and inorganic solvents, which suggested a similar chemical composition. The green color of the vanadium precipitate is attributed to the +3 oxidation state, prevalent in most green vanadium compounds [20]. However, the grey color of the precipitate obtained from mineral ore AMIS 0501 was presumed to be the result of the coprecipitation of other major elements in the sample.

Fusion using sodium phosphate flux in both samples resulted in clear solutions, with no traces of precipitates. This disparity of results prompted a further investigation to determine the influence of cations in the flux (Na^+ and NH_4^+) for the formation of a precipitate. Interestingly, all the resultant solutions after fusion using ammonium phosphate flux and sodium phosphate fusion had the same range of pH (1.2–1.8), which suggested that precipitation was not influenced by pH. The filtrate solution obtained after fusion with sodium phosphate solution was analyzed using ICP-MS, whilst the precipitates obtained using ammonium phosphate flux were characterized using IR, SEM-EDX, and XRD to determine the chemical composition.

3.1. IR Characterization

The IR analyses of the precipitates from V_2O_3 and AMIS 0501 mineral ore (Figure 1) were compared to determine any similarities in the stretching frequencies. Both spectra showed strong prominent peaks in the region of 1260–1240 cm^{-1}, which are characteristic of the P-O_{ext} stretching vibration of metaphosphates. The symmetrical stretching frequencies in the region of 1100–955 cm^{-1} were assigned to the (P-O)PO_2, whilst the stretching frequencies in the region of 765–705 cm^{-1} were assigned to the stretching mode of the P-O-P bridge bonds [21]. The similarities between the two spectra pointed to the presence of metaphosphate compounds in both precipitates. However, the variation in the stretching frequencies between the two spectra suggested the presence of two or more different metaphosphate compounds in the AMIS 0501 precipitate.

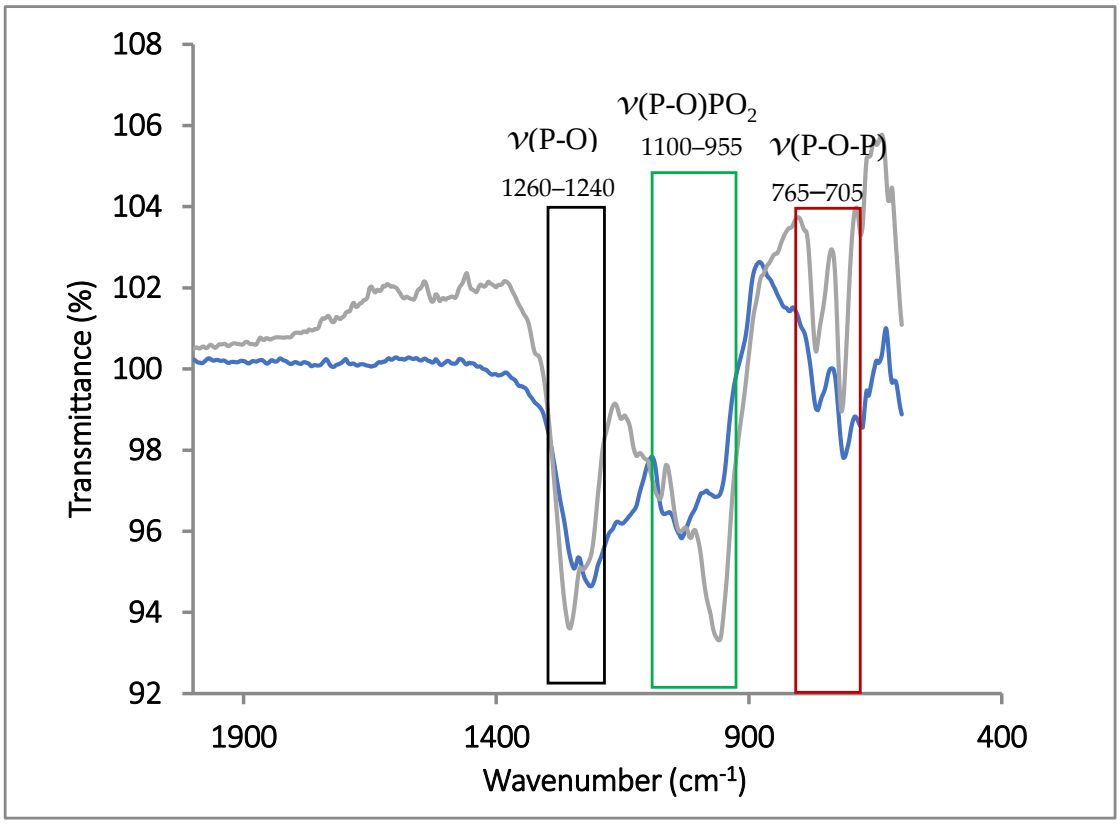

Figure 1. Infrared spectra of precipitates obtained after fusion of V_2O_3 and AMIS 0501 mineral ore with ammonium phosphate salt as flux.

It is worth noting the existence of iron and titanium metaphosphate compounds, which also exhibited similar stretching frequencies as metaphosphates of vanadium. A preliminary investigation of other additional phases present in the isolated products was carried out by comparing the stretching frequencies of Fe and Ti metaphosphate compounds with those reported in the literature [22], as shown in Table 2. It was identified that the IR spectra of the precipitate obtained from AMIS 0501 mineral ore had additional peaks, which suggested the presence of vanadium, titanium, and iron.

Table 2. Comparison of the stretching frequencies of metaphosphate compound $M(PO_3)_3$ where M = V, Fe, and Ti.

IR Stretching Bands	Ti	V	Fe
V_{as} (P − O_{ext}) | PO_2	1385 *vs*	**1240 *vs***	1230 *vs*
	1115 *s*	**1150 *s***	-
V_{as} (P − O_{int}) | P-O-P |	960 *s*	**975 *s***	970 *s*
	750 *m*	**765 *m***	750 *m*

vs—very strong, *s*—strong, *m*—medium, bold values—reflects the theme of the manuscript.

3.2. SEM-EDX and TEM Analyses

The SEM-EDX and TEM analyses were used to determine the morphological structure and the percentage composition of each element in the precipitates obtained from V_2O_3 and AMIS 0501 mineral ore. The SEM-EDX graphical images of the precipitate from V_2O_3 (Figure 2) showed microcrystalline, elongated crystal-like particles, which were uniform and clustered. The elemental composition of these microcrystalline particles was composed of mainly V, O, and P with the percentage weight content in the order of V(21 wt%) < P(35 wt%) < O(44 wt%). The TEM analysis also revealed the presence of three elements with percentage weight composition in the order of V(26 wt%) < P(56 wt%) < O(18 wt%). No other particles were detected in the precipitate obtained from V_2O_3. The average percentage weight ratio of 3:5:6 and 3:6:2 for V, O, and P pointed to the chemical formula of either a phosphate polymer or a phosphate compound ($V_3P_5O_6$ and $V_3P_6O_2$). The results were consistent with the IR predictions of a metaphosphate product.

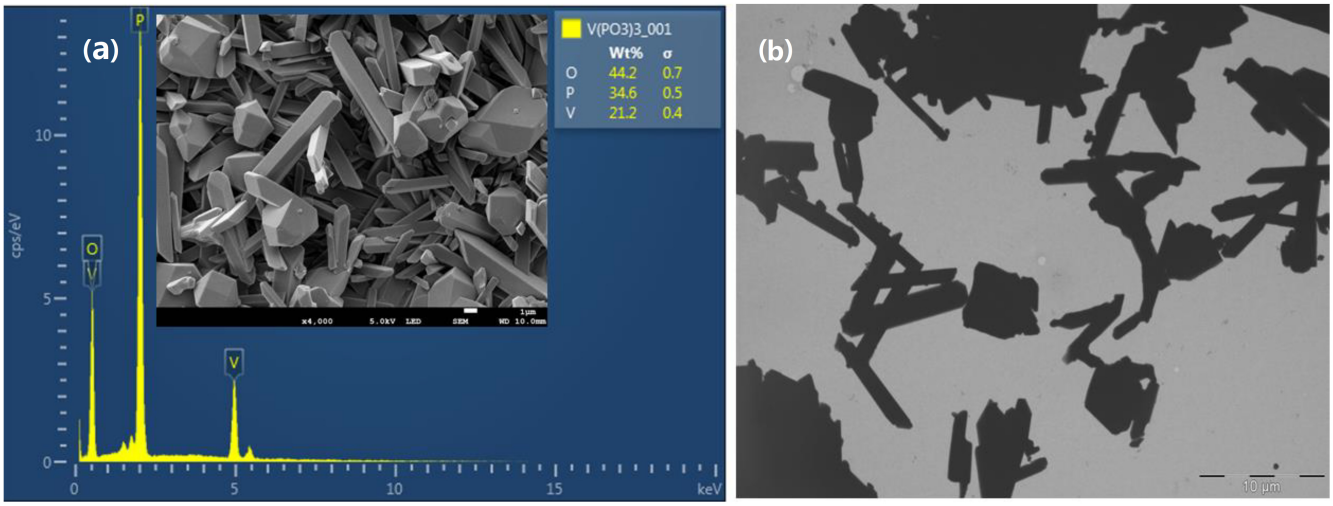

Figure 2. (**a**) SEM-EDX results and (**b**) TEM graphical images of the vanadium precipitate obtained from fusing ammonium phosphate with vanadium oxide (V_2O_5).

The SEM-EDX analysis (Figure 3) of the original AMIS 0501 mineral ore sample was analyzed first to determine the elemental composition as well as the morphological structure. The SEM images of the AMIS 0501 mineral ore sample revealed two microscopic levels of color contrast, with one bearing larger and greyish particles, whilst the other was lighter and smaller in size. Both particles appeared irregular and amorphous and showed varying amounts of Fe, Ti, and V, which suggests the presence of more than one phase in the ore. The larger greyish particles contained 64.3 wt% (Fe), 9.0 wt% (Ti), and 1.2 wt% (V) compared with the smaller lighter particles, with 48.1 wt% (Fe), 7.5 wt% (Ti), and 0.9 wt% (V). Iridium peaks, as detected in all EDX spectra, were from the double-sided tape that was used for sample mounting.

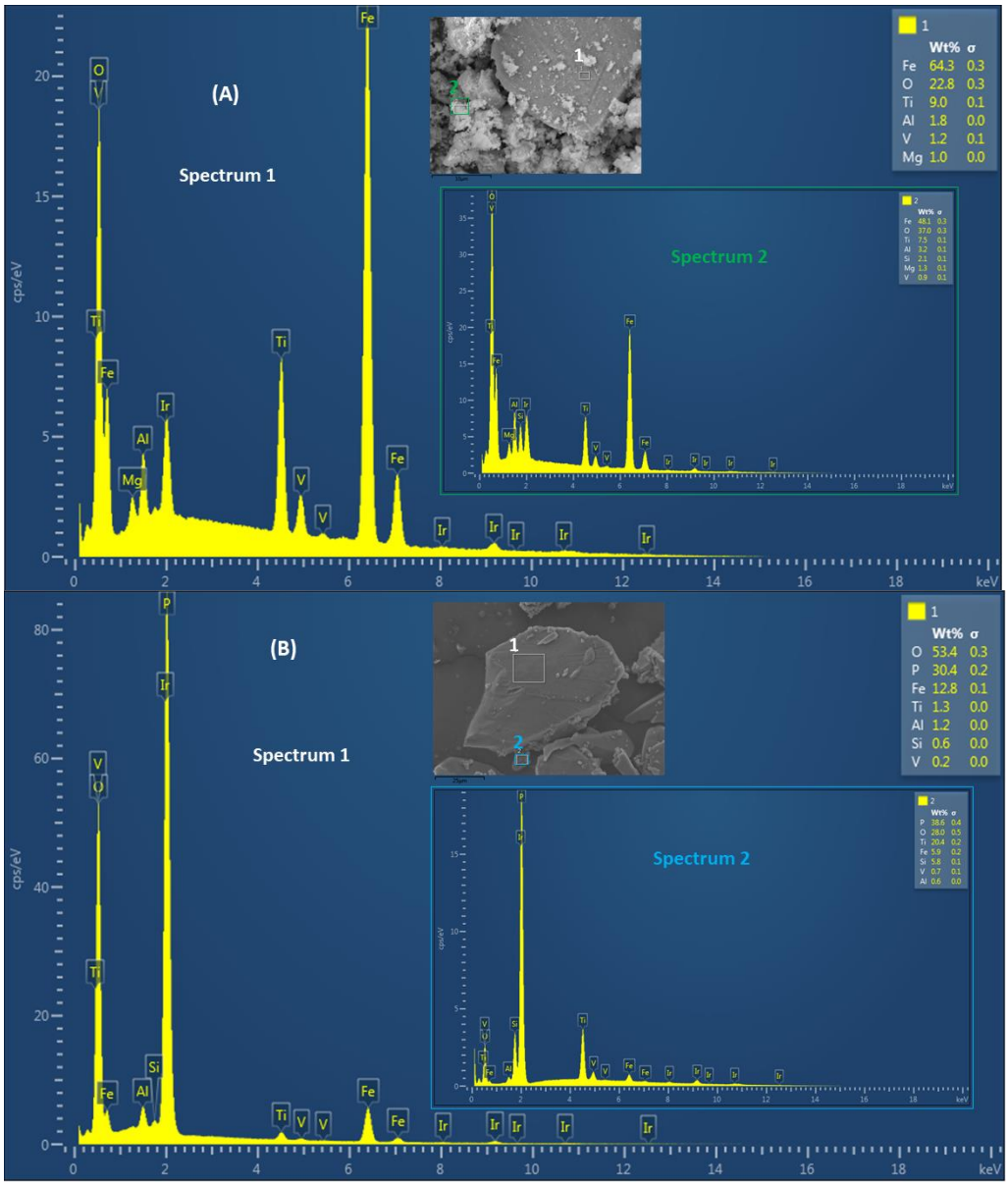

Figure 3. SEM-EDX graphical images and elemental results of (**A**) the original AMIS 0501 mineral ore sample and (**B**) precipitate isolated using ammonium phosphate flux.

The isolated precipitate from AMIS 0501 mineral ore (see Figure 3) revealed two distinct microscopic particles with different shapes and sizes. Both particles were amorphous and dark with varying elemental content of Fe, Ti and V. The larger particles had 12.8 wt% (Fe), 1.3 wt% (Ti), and 0.2 wt% (V) content compared with the smaller particles, which had 5.9 wt% (Fe), 20.4 wt% (Ti), and 0.7 wt% (V). The presence of vanadium in the AMIS precipitate confirmed the feasibility of this method for the isolation of vanadium in mineral ores. However, the specificity of this technique was compromised by the presence of impurities such as Fe, Ti, and Al, which have the potential to form metaphosphate compounds. The SEM-EDX also confirmed the IR results, which pointed to the presence of multiple metaphosphate products in the AMIS 0501 precipitate.

3.3. XRD Characterization

The XRD analysis was performed to determine the precise chemical composition and phase purity of the vanadium precipitate obtained from pure V_2O_3. The XRD pattern of the vanadium precipitate matched precisely with the monoclinic phase of vanadium(III)

tris(metaphosphate) ($V(PO_3)_3$) compound (JCPDS No. 01-072-2445), which belongs to the *Ic* space group. No additional peaks were observed for the XRD pattern of the precipitate other than the monoclinic phase, which confirmed the purity of the vanadium product.

The crystallite size (D) of vanadium(III) tris(metaphosphate) precipitate was determined using the Debye–Scherrer equation (Equation (1)), which showed a crystallite size range of 42–68 nm with an average size of 58 nm.

$$\text{Crystal size (D)} = \frac{0.9\,\lambda}{\beta \cos\theta} \quad (1)$$

where λ is the X-ray wavelength, β is the line broadening at half the maximum intensity (full width at half maximum, (FWHM)), and θ is the Bragg angle.

The monoclinic structure of the identified vanadium(III) tris(metaphosphate) product was confirmed by using the Rietveld refinement method. Lattice parameters, atomic position, site occupancy atoms, and unit cell volume were calculated from the Rietveld refinement. The crystallographic structure of the vanadium(III) tris(metaphosphate) compound is represented in Figure 4, and the structural refinement parameters are shown in Table 3. The theoretically calculated patterns ($Y_{Calculated}$) in refinement were well-matched with the experimentally observed XRD patterns (Figure 4a) ($Y_{Observed}$). The difference between the two profiles ($Y_{Observed} - Y_{Calculated}$) was about zero, shown by a line. The experimentally observed and calculated profiles are shown in Figure 4b. The excellent fitting parameter values of R_p, $R_{exp,}$ R_{wp}, and χ^2 refined values showed satisfactory structural refinement. The structural refinement analysis confirmed the monoclinic crystal structure having space group *Ic*.

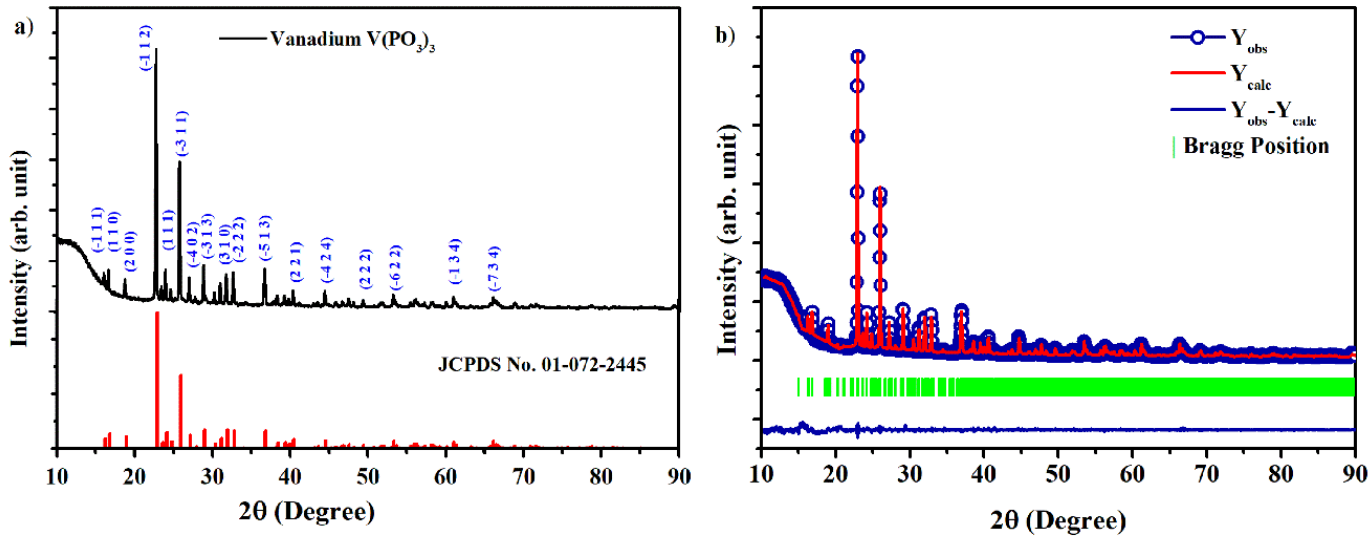

Figure 4. (**a**) XRD pattern and (**b**) Rietveld refinement fitting of vanadium(III) tris(metaphosphate).

In the crystal structure (Figure 5), the VO_6 group formed an octahedral with six neighboring oxygen atoms. Three different V sites formed three different octahedral structures with different bond lengths. The bond lengths were not equal in all the octahedral structures. The values of the calculated bond lengths are given in Table 4. The structural values such as lattice parameters and the bond length of the refined structure matched precisely with the reported structure by Middlemiss et al. [23]. It can be concluded that this fusion procedure using ammonium phosphate flux did not alter the structure of the product.

Table 3. Rietveld structural refinement parameters.

Bragg R-factor: 7.628 **RF-factor: 4.886** **χ^2 = 1.8** **a = 10.6071 Å** **b = 19.0871 Å** **c = 9.4230 Å** **α = 90.00, β = 97.93, γ = 90.00** **Volume = 1889.53 Å ^{3}**				
Atom	**x**	**y**	**Z**	**occ.**
O1	0.9606	0.4774	0.7353	1
O2	0.1184	0.1437	0.1921	1
O3	0.0451	0.9478	0.4205	1
O4	0.2627	0.0734	0.0379	1
O5	0.8387	0.6740	0.7283	1
O6	0.8384	0.6370	1.0028	1
O7	0.3241	0.4917	0.1643	1
O8	0.9314	0.7490	0.6261	1
O9	0.1485	0.3568	0.3185	1
O10	0.2382	0.3857	0.0778	1
O11	0.8794	0.9728	0.6960	1
O12	1.0033	0.9995	1.0429	1
O13	0.1074	0.8120	0.2309	1
O14	0.9555	0.1783	0.8031	1
O15	0.2598	0.7044	−0.0617	1
O16	0.1560	0.6733	0.3040	1
O17	0.8098	0.2520	0.9836	1
O18	0.8033	0.3008	0.9017	1
O19	0.0569	0.2239	0.3839	1
O20	0.9486	0.6831	0.0136	1
O21	−0.00014	0.5488	0.3091	1
O22	0.9612	0.3667	0.00046	1
O23	0.0020	0.9172	0.3857	1
O24	−0.1299	0.9669	0.1112	1
O25	0.9772	0.8025	0.7203	1
O26	0.9405	0.4315	0.5962	1
O27	0.8728	0.1198	0.6633	1
P1	1.0193	0.1479	0.7734	1
P2	0.1134	0.5182	0.6824	1
P3	0.0405	0.8317	0.7301	1
P4	0.0928	0.3160	0.4469	1
P5	0.1109	0.6499	0.3943	1
P6	0.1185	0.9720	0.4440	1
P7	0.8827	0.7015	0.5589	1
P8	0.9062	0.3715	0.5551	1
P9	0.8018	0.0448	0.4517	1
V1	0.2435	0.0738	0.2282	1
V2	0.2463	0.4031	0.2250	1
V3	0.2307	0.7520	0.2681	1

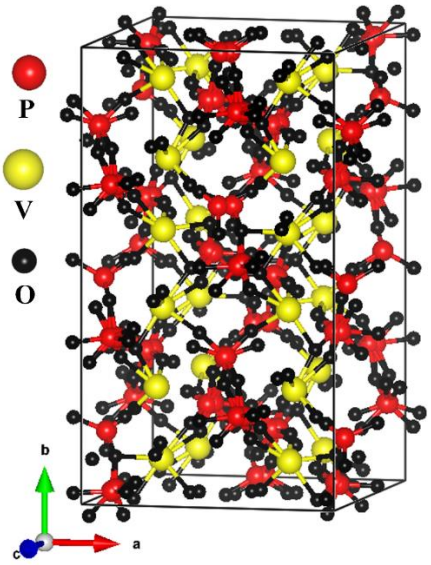

Figure 5. Crystallographic structure of the vanadium(III) tris(metaphosphate) compound.

Table 4. V-O bond length in the $V(PO_3)_3$ crystal structure.

$V(1)O_6$ Octahedral	$V(2)O_6$ Octahedral	$V(3)O_6$ Octahedral
Bond Length (Å) V(1)−O	**Bond Length (Å) V(2)−O**	**Bond Length (Å) V(3)−O**
1.80	1.74	1.70
1.82	1.75	1.74
1.83	1.82	1.78
1.84	1.88	1.81
1.88	2.04	1.99
1.97	2.09	2.00

3.4. Proposed Formation of Vanadium(III) Tris(Metaphosphate) and ICP-OES Analysis of the Filtrate Solutions

The formation of vanadium(III) tris(metaphosphate) was postulated to occur according to Equations (2) and (3). The decomposition of ammonium phosphate flux at 800 °C resulted in the release of ammonium gas, which might have triggered the formation of $V(PO_3)_3$ through the lowering of the pH (1.2–1.8). However, the lack of precipitation using sodium phosphate flux was attributed to the presence of Na^+ ions, which might have rendered the product soluble. The pungent smell noted during the fusion with ammonium phosphate salt suggested the release of NH_3 gas from the ammonium salt, which did not occur with the sodium phosphate analogue. It was postulated that the presence of trivalent ions (M^{3+}) in the solution could also result in the formation of a mixture of metaphosphate ($M(PO_3)_3$) products, as was the case of the precipitate obtained from the AMIS 0501 mineral ore.

$$(NH_4)H_2PO_4 \xrightarrow{\Delta\ (800\ ^\circ C)} PO_3^- + NH_3 \uparrow + H^+ \quad H_2O(\mathrm{pH} = 1.2 - 1.4) \tag{2}$$

$$3PO_3^- + V^{3+} \rightarrow V(PO_3)_3 \downarrow \tag{3}$$

The quantitative analysis of the filtrate solution obtained after the fusion of V_2O_3 with ammonium phosphate showed the presence of trace amounts of vanadium (<1.0%), which remained in the solution. This low vanadium content in the filtrate solution revealed the successful conversion of V_2O_3 into a metaphosphate product. The elemental analysis of vanadium content from V_2O_3 in the precipitate showed a remarkable recovery of 98%. However, a fair amount of vanadium (70%) was recovered in the precipitate obtained from

AMIS 0501 mineral ore, whilst the remaining amount (~30%) was recovered in the filtrate solution. It is highly plausible that the precipitation of vanadium was more selective to ions in the trivalent oxidation state, and vanadium ions with different oxidation states were retained in the solution. A summary of the quantitative analysis results of the liquid filtrate solutions is shown in Table 5.

Table 5. Elemental content of the sample filtrate solutions obtained after fusion using ammonium and sodium phosphate flux.

	Ammonium Phosphate flux (%)		
V_2O_3	**V**	**Ti**	**Fe**
Precipitate	98.5	-	-
Filtrate	<1.0	-	-
	Sodium phosphate flux (%)		
V_2O_3	**V**	**Ti**	**Fe**
Precipitate	-	-	-
Filtrate	99.3	-	-
	Ammonium phosphate flux (%)		
AMIS (0501) mineral ore	**V**	**Ti**	**Fe**
Precipitate	70.06	44.97	20.97
Filtrate	29.56	54.66	78.84
	Sodium phosphate flux (%)		
AMIS (0501) mineral ore	**V**	**Ti**	**Fe**
Precipitate	-	-	-
Filtrate	96.86	92.44	96.05

- Element not detected.

4. Conclusions

The isolation of vanadium(III) tris(metaphosphate) from an inorganic compound (V_2O_3) was achieved using ammonium phosphate salt as flux. The crystalline product was confirmed using XRD analysis. No additional peaks in the XRD pattern were present, which confirmed the purity of the product. This technique is assumed to be effective in extracting elements with trivalent oxidation states. However, the results obtained in this study also showed that this technique is affected by Fe, Ti, and Al, which have the ability to form trivalent ions. Due to its reported magnetic properties, the vanadium(III) tris(metaphosphate) product might be used in anticorrosive pigments, heterogeneous catalysis, ionic exchange, optoelectronics, glass host laser, and optical amplifier technologies [24,25].

Funding: This research received no external funding.

Acknowledgments: The authors would like to thank the Research Fund of the University of the Free State, South Africa, for financial support.

Conflicts of Interest: The author declares that they have no conflict of interest.

References

1. Fischer, R.P. *Geological Survey Professional Paper*; 926-B; United States Government Printing Office: Washington, DC, USA, 1975.
2. Reynolds, I.M. Mineralogical studies of South Africa titaniferous iron ores, their application to extractive metallurgy. *Trans. Geol. Soc. S. Afr.* **1978**, *81*, 233–240.
3. Langeslay, R.R.; Kaphan, D.M.; Marshall, C.L.; Stair, P.C.; Delferro, M. Catalytic applications of vanadium: A mechanistic perspective. *Chem. Rev.* **2018**, *119*, 2128–2191. [CrossRef] [PubMed]
4. Pourret, O.; Dia, A. Vanadium. In *Encyclopedia of Geochemistry*; White, W.M., Ed.; Springer: Cham, Switzerland, 2016. [CrossRef]
5. Doetsch, C.; Burfeind, J. Vanadium redox flow batteries. In *Storing Energy*, 2nd ed.; Elsevier: Amsterdam, The Netherlands, 2022; pp. 363–381. ISBN 9780128245101.
6. Barnes, A.R.; Newall, A.F. *Spinel Removal from PGM Smelting Furnaces*; South African Institute of Mining and Metallurgy: Johannesburg, South Africa, 2006; pp. 77–88.

7. Dai, Z.; Guan, D.; Liu, Y.; Hu, D.; Zhou, R.; Cao, J.; Cheng, L.; Pu, X. Acid leaching process in extracting vanadium from blast furnace slag in Panzhihua vanadium titanium magnetite. In *Advances in Energy and Environmental Materials, Proceedings of the Chinese Materials Conference, Yinchuan, China, 18 April 2017*; Springer: Singapore, 2018. [CrossRef]
8. Lekobotja, M.; Mojapelo, M.; Goso, X.C.; Lagendijk, H. Recovery of vanadium from discard titaniferous magnetite slag using the soda ash roast-leach process. In Proceedings of the 3rd Young Professionals Conference, Pretoria, South Africa, 9–10 March 2017.
9. Lee, J.-C.; Kurniawan; Kim, E.-Y.; Chung, K.W.; Kim, R.; Jeon, H.-S. A review on the metallurgical recycling of vanadium from slags towards a sustainable vanadium production. *J. Mater. Res. Technol.* **2021**, *12*, 343–364. [CrossRef]
10. Wang, M.; Chen, B.; Huang, S.; Wang, X.; Liu, B.; Ge, Q.; Xie, S. A novel technology for vanadium and chromium recovery from V-Cr-bearing reducing slag. *Hydrometallurgy* **2017**, *171*, 116–122. [CrossRef]
11. Jing, X.; Ning, P.; Cao, H.; Wang, J.; Sun, Z. High-performance recovery of vanadium (V) in leaching/aqueous solution by a reusable reagent-primary amine N1519. *ACS Sustain. Chem. Eng.* **2017**, *5*, 3096–3102. [CrossRef]
12. Gupta, V.K.; Ali, I.; Saleh, T.A.; Siddiqui, M.N.; Agarwal, S. Chromium removal from water by activated carbon developed from waste rubber tires. *Environ. Sci. Pollut. Res.* **2013**, *20*, 1261–1268. [CrossRef] [PubMed]
13. Chiweshe, T.T.; Purcell, W.; Venter, J.A. Evaluation of PGM liberation and chromium isolation in a solid UG2 chromitite concentrates at moderate temperatures using ICP-OES. *JOM* **2016**, *68*, 1691–1700. [CrossRef]
14. Gruss, M.; Glaum, R. Refinement of the superstructure of c-type chromium(III) tris(metaphosphate), $Cr(PO_3)_3$. *Acta Cystallogr. Sect. C.* **1996**, *52*, 2647–2650. [CrossRef]
15. Chiweshe, T.T.; Potgieter-Vermaak, S.; Purcell, W. Characterization of chromium(III) compounds Isolated from different mineral ores using ammonium phosphate flux. *Min. Metall. Explor.* **2018**, *33*, 441–450. [CrossRef]
16. Haushalter, R.C.; Mundi, L.A. Reduced molybdenum phosphate: Octahedral-tetrahedral framework solids with tunnels, cages and micropores. *Chem. Mater.* **1992**, *4*, 31–48. [CrossRef]
17. Ilieva, D.; Kovacheva, D.; Petkov, C.; Bogachev, G. Vibrational spectra of $R(PO_3)_3$ metaphosphates (R = Ga, In, Y, Sm, Gd, Dy). *J. Raman Spectrosc.* **2001**, *32*, 893–899. [CrossRef]
18. Elbouaanani, L.K.; Malaman, B.; Gérardin, R. Structure Refinement and Magnetic Properties of C–$Fe(PO_3)_3$ Studied by Neutron Diffraction and Mössbauer Techniques. *J. Solid State Chem.* **1999**, *148*, 455–463. [CrossRef]
19. Education.com, Inc., a Division of IXL Learning. Available online: https://www.education.com/science-fair/article/mohs-hardness-test-minerals/ (accessed on 17 August 2022).
20. Mwakikunga, B.W. Vanadium Metal and Compounds, Properties, Interactions, and Applications. In *Encyclopedia of Metalloproteins*; Kretsinger, R.H., Uversky, V.N., Permyakov, E.A., Eds.; Springer: New York, NY, USA, 2013. [CrossRef]
21. Stuart, B.H. *Infrared Spectroscopy: Fundamentals and Applications*; John Wiley & Sons: Hoboken, NJ, USA, 2004; p. 84.
22. Rojo, J.M.; Pizarro, J.L.; Rodríguez Fernández, J.; Greneche, J.M.; Arriortua, M.I.; Fernández-Díaz, M.T.; Rojo, T. Magnetic properties of $M(PO_3)_3$ (M = Fe, Mo). A comparative neutron diffraction study. *J. Mater. Chem.* **2003**, *13*, 1723–1730. [CrossRef]
23. Middlemiss, N.; Hawthorne, F.; Calvo, C. Crystal structure of vanadium(III) tris(metaphosphate). *Can. J. Chem.* **1977**, *55*, 1673–1679. [CrossRef]
24. Durville, F.M.; Behrens, E.G.; Powell, R.C. Laser-Induced refractive index gratings in Eu-doped glasses. *Phys. Rev. B Condens. Matter* **1986**, *34*, 4213–4220. [CrossRef]
25. Broer, M.; Bruce, A.; Grodkiewicz, W. Photoinduced refractive-index changes in several Eu^{3+}, Pr^{3+} and Er^{3+} doped oxide glasses. *Phys. Rev. B* **1992**, *45*, 7077. [CrossRef]